Elastic properties of dry clay mineral aggregates, suspensions and sandstones

Tiziana Vanorio,* Manika Prasad and Amos Nur

Stanford Rock Physics Laboratory, Stanford University, CA 94305-2215, USA. E-mail: vanorio@geoazur.unice.fr

SUMMARY

The presence of clay minerals can alter the elastic behaviour of rocks significantly. Although clay minerals are common in sedimentary formations and seismic measurements are our main tools for studying subsurface lithologies, measurements of elastic properties of clay minerals have proven difficult. Theoretical values for the bulk modulus of clay are reported between 20 and 50 GPa. The only published experimental measurement of Young's modulus in a clay mineral using atomic force acoustic microscopy (AFAM) gave a much lower value of 6.2 GPa. This study has concentrated on using independent experimental methods to measure the elastic moduli of clay minerals as functions of pressure and saturation. First, ultrasonic *P*- and *S*-wave velocities were measured as functions of hydrostatic pressure in cold-pressed clay aggregates with porosity and grain density ranging from 4 to 43 per cent and 2.13 to 2.83 g cm^{-3}, respectively. In the second experiment, *P*- and *S*-wave velocities in clay powders were measured under uniaxial stresses compaction. In the third experiment, *P*-wave velocity and attenuation in a kaolinite–water suspension with clay concentrations between 0 and 60 per cent were measured at ambient conditions. Our elastic moduli measurements of kaolinite, montmorillonite and smectite are consistent for all experiments and with reported AFAM measurements on a nanometre scale. The bulk modulus values of the solid clay phase (K_s) lie between 6 and 12 GPa and shear (μ_s) modulus values vary between 4 and 6 GPa. A comparison is made between the accuracy of velocity prediction in shaley sandstones and clay–water and clay–sand mixtures using the values measured in this study and those from theoretical models. Using $K_s = 12$ GPa and $\mu_s = 6$ GPa from this study, the models give a much better prediction both of experimental velocity reduction due to increase in clay content in sandstones and velocity measurements in a kaolinite–water suspension.

Key words: acoustic velocities, clay minerals, elastic moduli, porosity.

1 INTRODUCTION

Elastic properties of clay minerals are of great interest for exploration and characterization of shaley formations. Knowledge of elastic moduli of clay minerals is required because: (1) clay minerals are found in most sedimentary environments; (2) clay mineral transitions are considered as important factors in seismogenic zones; and (3) seismic interpretation and modelling seismic response requires knowledge on how the presence of clay changes the physical properties of rocks.

Laboratory data from several investigators (Tosaya 1982; Tosaya & Nur 1982; Kowallis *et al.* 1984; Han 1986; Klimentos 1991) report a systematic decrease of *P*- and *S*-wave velocity with increasing clay content in both well and poorly consolidated sediments. How-

ever, the empirical relations derived from these measurements are restricted to specific lithologies and thus resist generalization. On the other hand, the use of deterministic models to establishing porosity–velocity relations in shaley sandstones requires knowledge of input parameters such as elastic moduli of the solid clay phase.

Elastic properties of clay minerals are almost unknown, mainly because of the difficulty presented by their intrinsic properties. Their small grain size makes it impossible to isolate an individual crystal of clay large enough to measure acoustic properties; reactions with organic polar molecules (Theng 1974) affects handling and clay structure; and low permeability makes saturation difficult. So far the effective elastic properties of clays have been derived either by theoretical computation (Alexandrov & Ryzhova 1961; Berge & Berryman 1995; Katahara 1996), by a combination of theoretical and experimental investigations on clay–epoxy mixtures (Wang *et al.* 2001), or by empirical extrapolations from measurements on shales (Tosaya 1982; Castagna *et al.* 1995; Han 1986). These derived

*Now at: UMR Géosciences Azur, Université de Nice, Sophia Antipolis, France.

values of clay moduli show little agreement. The values reported by Katahara (1996) and Wang *et al.* (2001) (*ca.* 50 GPa for bulk modulus, K and 20 GPa for shear modulus, μ) are higher than those extrapolated (*ca.* 20 GPa for K and 7 GPa for μ) from both laboratory (Castagna *et al.* 1995; Han 1986; Tosaya 1982) and well log measurements in shales and laminated shaley-sands (Eastwood & Castagna 1987). Katahara (1996) explained this discrepancy by acoustic anisotropy: in shaley beds, clay particles tend to align parallel to bedding during compaction. Using theoretical models of shaley sandstones, Berge & Berryman (1995) have shown that the bulk modulus of clay should be around 10–12 GPa. Only one experimental measurement exists on pure clay minerals: Prasad *et al.* (2002) have reported measurements of Young's modulus on clay particles using atomic force acoustic microscopy. Their measured value of Young's modulus for dickite is 6.2 GPa.

We have made direct measurements of the elastic properties of clay minerals by designing experiments that took into account factors affecting clay structures. We used three independent experimental set-ups: (1) a method of obtaining dry clay aggregates having different porosities on which *P*- and *S*-velocity (V_p, V_s, respectively) measurements were made as functions of hydrostatic pressure; (2) V_p and V_s measurements on clay powder as functions of uniaxial stress; and (3) *P* velocity and attenuation (V_p and Q_p, respectively) measurements on water–clay suspension as functions of clay content.

The measurements of elastic moduli for the solid clay phase from all experiments are consistent with each other. In order to verify the reliability of results, the measured moduli values were used in effective medium and granular porous media models and compared with pre-existing data on shaley sandstones (Tosaya 1982; Han 1986; Klimentos 1991). We demonstrate that our measured values of the elastic moduli for clay can be used to predict velocity data in saturated kaolinite samples (Yin 1993), kaolinite–water suspensions (this study) and shaley sandstones (Tosaya 1982; Han 1986; Klimentos 1991).

2 EXPERIMENTAL PROCEDURES AND METHODS

2.1 Collection of clay samples

Samples used in this study were prepared from clay powders obtained from the repository of the Clay Minerals Society. Clay samples included: kaolinite (KGa-1b, reported in the paper as Ka1), Ca-montmorillonite (STx-1, reported as Ca-Mt), Na-montmorillonite (SWy-2, reported as Na-Mt), illite (IMt1, reported as Imt), smectite (SWa-1, reported as Sm) and chlorite (CCa-2, reported as Ch).

2.2 Methods

Our methods of measuring elastic moduli of solid clays were chosen taking into account the various factors affecting clay structures. Brace *et al.* (1969) and Chung (1979) have described a hot-pressing method to determine elastic properties of some mineral powders. This method cannot be used for clays because they are sensitive to temperature and pressure. As temperature increases, clays first dehydrate and then dehydroxylate changing, respectively, their adsorbed water content and their mineral structure. The dehydration temperature depends on pressure (Koster Van Groos & Guggenheim 1984; Colten Bradley 1987). Chemical reagents cannot be used for sample preparation because some clay minerals change structure due to

reaction with polar compounds. These reactions can be exothermic and the temperature may rise to such a level as to overheat the clay specimen (Theng 1974; Newman 1987). The effects of reactions on clay minerals depend largely on their structure (Theng 1974). The basal spacing of the $Si(O,OH)_4$-tetrahedra (T) and $M_{2-3}(OH)_6$-octahedra (O) layers (where M is either a divalent or a trivalent cation) as well as size, the valence and the charge of the embedded exchangable cations profoundly influence adsorption of polar molecules other than water. For example, kaolinite shows a fully collapsed structure that is wanting either in water molecules or in exchangable cations or both. In these structures, intercalation of polar organic liquids or gases is quite complex and adsorption occurs predominantly on the external crystal surfaces (Theng 1974). On the other hand, smectite-type minerals, which host both exchangable cations and water interlayers, adsorb polar organic molecules by replacing their water interlayers. During the internal adsorption, the organic compound competes with water for the same sites around the exchangable cation. The removal and replacement of the water interlayer can be so invasive as to provoke dissociation of clay layers (Theng 1974).

An understanding of how these factors affect acoustic measurements is lacking. Since all the above-mentioned effects alter the clay structure, we expect an accompanying change in elastic properties as well. To eliminate these secondary effects, we used the cold-pressing method in which measurements are conducted on pure clay powders pressed at ambient room temperatures. Relatively low-pressure conditions (up to 20 MPa) ensured that the applied pressures did not promote dehydration of the clay minerals. Similarly, in the suspension experiment, a KCl solution was used with kaolinite to limit the effects of adsorption of polar water molecules and the cation exchange capacity of the clay.

2.2.1 Porosity and grain density determination

The grain density of the clay powders was measured using a pycnometer. To avoid trapped air produced by clay flocculation, we used sodium hexametaphosphate in distilled water (40 g of solute/litre) as the dispersive agent (ASTM 1992). For the cold-pressed aggregate samples, porosity, bulk and grain densities were measured at room *P–T* conditions with a helium porosimeter (with a measurement error of about 1 per cent).

2.2.2 Cold-pressing experiment

Sample preparation. This set-up was designed to make clay aggregate samples from the powders described in Section 2.1. These samples were used for measurements of V_p and V_s as functions of hydrostatic pressure. The equipment consists of a split steel cube with a cylindrical cavity (Fig. 1). Two pistons on either side of this cavity are used to apply uniaxial stress on a powder placed in the cavity. Porous stones coupled to filter paper on either end prevented the samples from bonding to the endplates during the cold-pressing procedure. The split steel cube allows sample recovery without applying additional stress. Powders were cold-pressed at 15 MPa for 1, 7 and 10 d to obtain samples of different porosity. Porosity, density and acoustic properties were measured on these samples at ambient conditions and at different confining pressure (up to 20 MPa).

Acoustic measurements. A complete description of the experimental set-up used in this study can be found in Prasad & Manghnani (1997) and Vanorio *et al.* (2002). Measurements were performed by increasing the confining pressure up to 20 MPa with a pressure

Figure 1. Different stages of the cold-pressing procedure.

interval of 1 MPa. During the down cycle, measurements were taken with a pressure interval of ≈5 MPa. Three linear potentiometers were used to measure length changes of the samples as a function of stress. The length change was directly related to changes in porosity by assuming that pore collapse was the main cause of strain. This allowed computation of porosity change with pressure using initial porosity, grain density and length change. V_p and V_s were measured at each pressure step. Traveltime was measured after digitizing waveforms with 1024 points at a time sweep of 5 μs, thus allowing a time resolution of about 5 ns or about 0.2 per cent error in velocity. The actual error in velocity measurement is estimated to be around 1 per cent due to operator error in picking the first arrival time. The system delay time was measured by taking the head-to-head time at 2 MPa. The traveltime calibration was confirmed by measuring an aluminium sample at different pressures.

2.2.3 Uniaxial stress experiment

Samples preparation. Clay powder of kaolinite (KGa-1b), Na-montmorillonite (SWy-2) and Ca-montmorillonite (STx-1) were used for this experiment. The cold-pressing set-up was altered to allow the simultaneous measurement of acoustic velocities during the uniaxial stress compaction of clay powders. PZT crystals with a principal frequency of 1 MHz mounted on the piston endplates were used to generate *P* and *S* waves. A high-viscosity bonding medium (Panamterics SWC) was used to bond the endplates to the sample. Acoustic isolation from steel was achieved by jacketing the samples with rubber tubing.

Acoustic measurements. The experimental setup for the uniaxial pressure tests consisted of a digital oscilloscope (Tektronix TDS 420A) and a pulse generator (Panametrics 5052 PR). Measurements were performed by increasing pressure up to 20 MPa with a variable pressure interval from 2.5 to 5 MPa. A caliper was used to measure length changes of the samples as a function of stress (precision = ± 1 mm). The length measurements were made at eight positions around the plate in order to detect possible sample tilting. Computations of both porosity change and traveltime were made as described in Section 2.2.2. In this experiment, porosities might be underestimated due to deformation of the rubber jacket. However, comparison with our other results and the modelling in Section 4 show this deformation to be minimal. This assumption was further tested using a water sample in the uniaxial experiment because of its highest Poisson ratio value. The test demonstrated that the deformation of the rubber jacket led to a diameter expansion of 1.5 mm. Assuming a

similar behaviour for clays, this corresponds to a porosity error of less than 7 per cent.

2.2.4 Suspension experiment

Sample preparation. Clay powder of kaolinite (KGa-1b), a non-swelling clay, was used in the experiments to limit the effects of polar water molecule adsorption (Theng 1974). To further minimize swelling and the cation exchange capacity, the suspension was prepared in a degassed, 20 000 ppm KCl solution. The size of the K-ion radius, of the order of the kaolinite layer spacing, prevented both cation exchange (Theng 1974) and water molecules from bounding to any cation in the interlayer position. Measured amounts of clay were added to the water to allow computations of clay content and water saturation. To avoid clumps in the suspension, the powder was sieved before adding it to the water. Trapped air was minimized by constant stirring, shaking and by using vacuum to de-air the suspension. Acoustic measurements were performed while increasing clay content in the suspension from 0 to 60 per cent using a step of 2 per cent for clay contents less then 40 per cent, and a step of 5 per cent for clay content above 40 per cent. Measurements were discontinued for clay concentrations greater than 60 per cent: the sample was too viscous to permit a complete outgassing and velocity estimates would be biased by gas content.

Acoustic measurements. The experimental setup consisted of a Plexiglas container that held the kaolinite–water suspension (Fig. 2). Sealed holes on two sides of the container positioned the immersion transducers (1 MHz Panametrics Transducers V303-SU) in the kaolinite–water suspension. In order to avoid reflections from the container sides, the distance between immersion transducers (2.54 cm) was kept shorter than the dimensions of the Plexiglas container ($27 \times 10 \times 27$ cm^3). The distance between transducers was fixed during the measurements and was used for velocity computation. The transducers were excited using a Panametrics (5052 PR) pulser. The signals through the suspension were received and digitized by a digital Tektronix oscilloscope (TDS 420 A) and stored on a computer. At each clay concentration two signal acquisitions were taken to ensure the repeatability of measurements. The *P*-wave quality factor (Q_p) (±5 per cent) was calculated from the stored signal waveforms by the spectral ratio technique (Toksöz *et al.* 1979; Prasad & Manghnani 1997). The signal from the initial KCl water
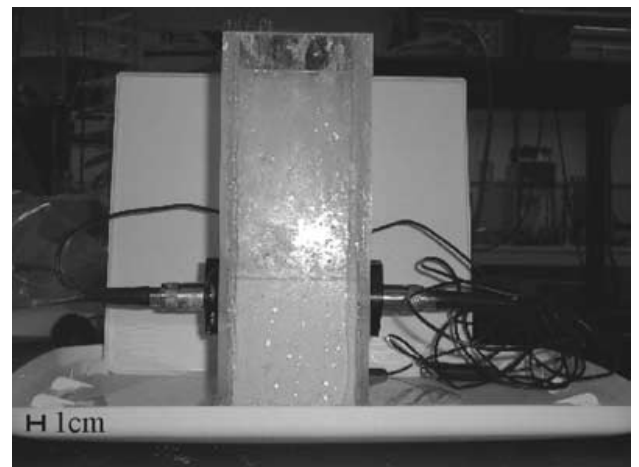

Figure 2. Suspension measurement equipment for kaolinite sample. Note that the active faces of the transducers are inside the container.

solution was recorded and used as a reference signal. In this way similar conditions were maintained for the reference and the sample.

3 RESULTS

3.1 Grain density, porosity and sample state

Table 1 compares grain and bulk density, and porosity values measured using the methods described in Section 2.2.1.

Differences in grain densities values for most of samples were less than 2 per cent except for Na-montmorillonite samples ($\approx$7 per cent). Swelling of this clay mineral, which affects the volume estimate, was noted during the measurement. For Na-montmorillonite samples we will refer to physical properties measured by the He-porosimeter.

Table 1 also shows that clay mineralogy controls both porosity and the state of samples obtained by the cold-pressing procedure described in Section 2.2.2. Upon removal of samples from the cold-pressing apparatus, well-compacted low-porosity ($4 < \Phi < 20$ per cent) samples of Na-, Ca-montmorillonite (Na-Mt, Ca-Mt), and smectite (Sm) were obtained (Fig. 3a). In contrast, illite (Imt) and chlorite (Ch) samples presented higher porosity ($20 < \Phi < 30$ per cent) and slowly deteriorated with microcracks forming perpendicular to the applied stress direction (for example, sample Ch in Fig. 3b). This effect was most pronounced in kaolinite samples, which completely disaggregated on removal from the housing apparatus (sample Ka1 in Fig. 3b). Since deterioration of samples was typical of clays without water interlayers, and it occurred both at room humidity and under vacuum (samples Ka1 and Ch), this behaviour could be related to clay mineralogy. This hypothesis was confirmed by cold-pressing two dehydrated powders from the smectite group which, in their natural hydrated state, produced good samples (Fig. 3a). Fig. 3(b) shows that the dehydrated Sm and Ca-Mt samples disaggregated upon the removal of the cold-pressing pressure. The results from the cold-pressing experiment show that water interlayers in the clay mineral structure play an important role in the compaction and strength of clay aggregates.

3.2 Acoustic measurements on cold-pressed samples under hydrostatic pressure

Because of the lowest porosity of the suite of studied samples, samples of smectite and Na-montmorillonite were used for the hydro-
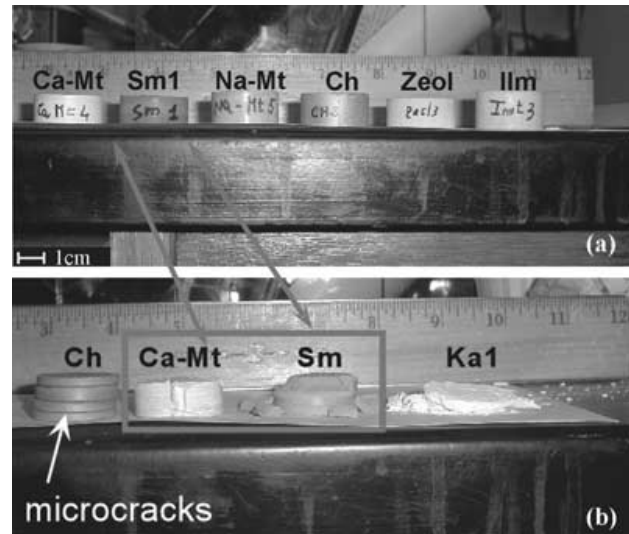

Figure 3. (a) Aggregated samples of clay minerals obtained by the cold-pressing procedure: kaolinite (Ka), chlorite (Ch), Na-montmorillonite (Na-Mt), Ca-montmorillonite (Ca-Mt), smectite (Sm), illite (Imt), zeol (zeolites); (b) samples completely disaggregated upon removal of cold-pressing pressure (Ka1) and with microcracks formed perpendicular to the applied stress direction (sample Ch). In the box, samples of dehydrated Sm and Ca-Mt are shown disaggregated upon the removal of cold-pressing pressure (b). Arrows connect the same powders in their natural and in dehydrated states.

static pressure experiment. The experiment was repeated on different samples to ensure repeatability of measurements. In Figs 4 and 5, measurements of velocity and elastic moduli are reported for the smectite sample as functions of pressure and porosity, respectively. Because of the initial low porosity of the smectite sample (4.5 per cent), it was possible to measure velocities and elastic moduli at porosities as low as 0.8 per cent at a confining pressure of 20 MPa. Extrapolation using a polynomial fit to the data (Table 2) shows that, at 0 per cent porosity, $V_p = 2.3$ km s^{-1}, $V_s = 1.3$ km s^{-1}, $K = 6$ GPa and $\mu = 4$ GPa. Fig. 4 shows that velocity values measured during unloading are higher than those measured during increasing pressure. Although the sample is allowed to re-equilibrate after pressure release, porosity is not readily recovered in clay and, as consequence, the velocity is higher. As pressure decreases, this effect is less evident since the sample has had enough time to re-equilibrate; below 5 MPa the time-lag in recovering of porosity is less pronounced.

Table 1. Porosity, bulk (ρ_b) and grain density (ρ_g) of cold-pressed clay samples.

| Sample	Pycnometer			He-porosimeter			Sample	Pycnometer			He-Porosimeter		
	ρ_g (g cm^{-3})	Φ (per cent)	ρ_b (g cm^{-3})	ρ_g (g cm^{-3})	Φ (per cent)	ρ_b (g cm^{-3})		ρ_g (g cm^{-3})	Φ (per cent)	ρ_b (g cm^{-3})	ρ_g (g cm^{-3})	Φ (per cent)	ρ_b (g cm^{-3})
Ka1	2.59	43	1.48	Nm^a	Nm	Nm	Sm3	2.29	6	2.15	2.28	6	2.15
Ka2	2.59	43	1.48	Nm	Nm	Nm	Sm4	2.29	4	2.19	2.30	5	2.19
Na-Mt1	2.30	13	2.00	2.47	11	2.19	Sm5	2.29	22	1.80	2.30	22	1.80
Na-Mt2	2.30	9	2.09	2.44	10	2.19	Sm6	2.29	10	2.05	2.29	10	2.05
Na-Mt3	2.30	14	1.99	2.47	20	1.99	Ca-Mt-1	2.13	22	1.68	2.14	22	1.68
Na-Mt4	2.30	12	2.02	2.48	18	2.02	Ca-Mt-2	2.13	21	1.69	2.13	21	1.69
Na-Mt5	2.30	11	2.05	2.47	17	2.05	Ca-Mt-3	2.13	17	1.76	2.13	17	1.76
Na-Mt6	2.30	19	1.85	2.47	25	1.85	Ca-Mt-4	2.13	21	1.67	2.12	21	1.67
Sm1	2.29	8	2.11	2.29	7	2.13	CH3	2.83	25	2.03	Nm	Nm	Nm
Sm2	2.29	13	1.99	2.29	13	1.99	Imt1	2.68	22	2.10	Nm	Nm	Nm

Nm = samples not measurable.
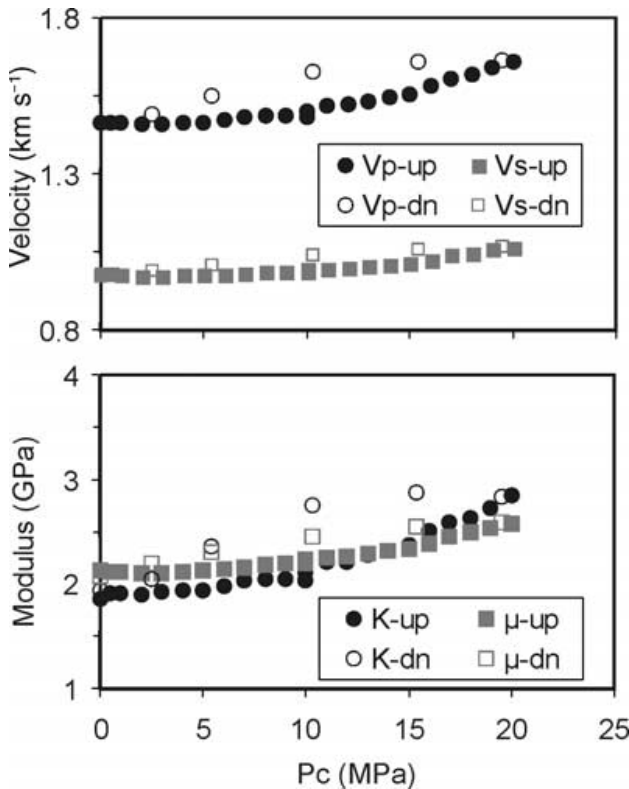
Figure 4. Velocity (a) and elastic moduli (b) as functions of hydrostatic pressure for smectite. Solid symbols mark increasing and open symbols mark decreasing pressures. The error on velocity is 1 per cent; the error bar in the velocity plots is smaller than the size of the symbols.
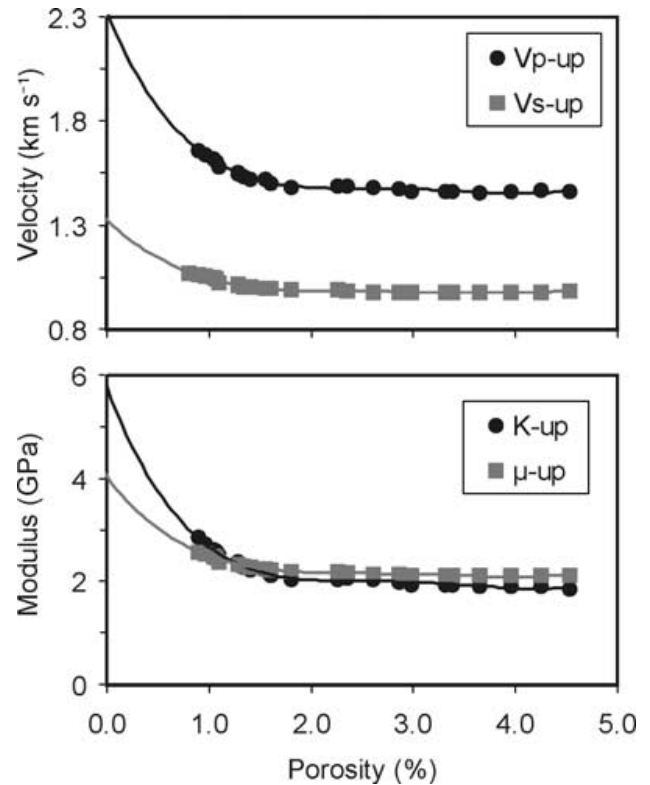

Figure 5. Velocity (a) and elastic moduli (b) as functions of porosity for the smectite. Lines show polynomial fits to the data: $M = a\Phi^4 + b\Phi^3 + c\Phi^2 + d\Phi + e$, where Φ = porosity.

Table 2. Coefficients of polynomial curves fit to the data.

Smectite	$M = a\Phi^4 + b\Phi^3 + c\Phi^2 + d\Phi + e$					
M	a	b	c	d	e	R^2
V_p	0.011	−0.138	0.613	−1.184	2.321	(0.986)
V_s	0.005	−0.054	0.242	−0.471	1.324	(0.979)
K	0.026	−0.310	1.355	−2.603	5.75	(0.984)
μ	0.049	−0.601	2.682	−5.212	4.02	(0.988)
Kaolinite and Na-Montmorillonite			$M = a\Phi + b$			
M	a	b	R^2	a	b	R^2
V_p	−0.03	2.695	(0.971)	−0.05	2.748	(0.974)
V_s	−0.01	1.436	(0.952)	−0.02	1.496	(0.956)
K	−0.21	11	(0.967)	−0.35	11	(0.994)
μ	−0.10	6	(0.969)	−0.15	5.5	(0.990)

3.3 Acoustic measurements under the uniaxial stress condition

In this experiment we monitored velocity and elastic moduli variations during uniaxial stress compaction of kaolinite and Na-montmorillonite powders. Fig. 6 shows the variations in velocity and elastic moduli as functions of porosity for kaolinite (Ka1) and montmorillonite (Na-Mt) in dry condition. At the lowest porosity, a linear fit to the data gives elastic moduli for kaolinite mineral as 11 GPa for K and 6 GPa for μ, respectively. Measurements on Na-montmorillonite provided moduli of 11 GPa for K and 5.5 GPa for μ (Table 2). The different trends shown in the hydrostatic and uniaxial stress compaction experiments could be due to the dissimilar aggregation state of the samples used. In the uniaxial experiment, we capture the entire compaction curve from the clay powder, having negligible pore stiffness, to very low porosity aggregate, whereas in the hydrostatic case, since we have pre-compressed the Sm sample, we are looking at the lowermost porosity of the compaction curve. Future measurements will show whether and how the velocity–porosity trend deviates from linearity at very low porosity.

3.4 Acoustic measurements in kaolinite–water suspension

Fig. 7 shows the variation of bulk modulus (Fig. 7a) and quality factor (Fig. 7b) as functions of clay content in the suspension. The bulk modulus was calculated from V_p and density measurements by assuming $\mu = 0$, that is, the shear wave did not propagate through the suspension. In Fig. 7(a), at clay concentrations below 40 per cent, the bulk modulus (K) increases slightly with increasing clay

content. Beyond 40 per cent there is a change in the slope of the bulk modulus increase. In Fig. 7(b), the P-wave quality factor (Q_p) decreases with increasing clay content and reaches a minimum at 40 per cent clay concentration. After this minimum, Q_p increases with increasing clay concentration.

The behaviour of K as a function of increasing clay content is similar to the results of V_p in clay—sand mixtures reported by Marion *et al.* (1992). Marion *et al.* (1992) show that when clay volume fraction (C) is less than 0.4–0.45 (as in Fig. 7a), clay particles are suspended in the pore space of the load-bearing medium (sand in their case, water in this study) and velocity measurements reflect mainly a density effect. Q_p decreases due to scattering at possible clumping of the clay. At clay volume fractions greater than 0.4–0.45, clay becomes the load-bearing phase and water (or sand) becomes
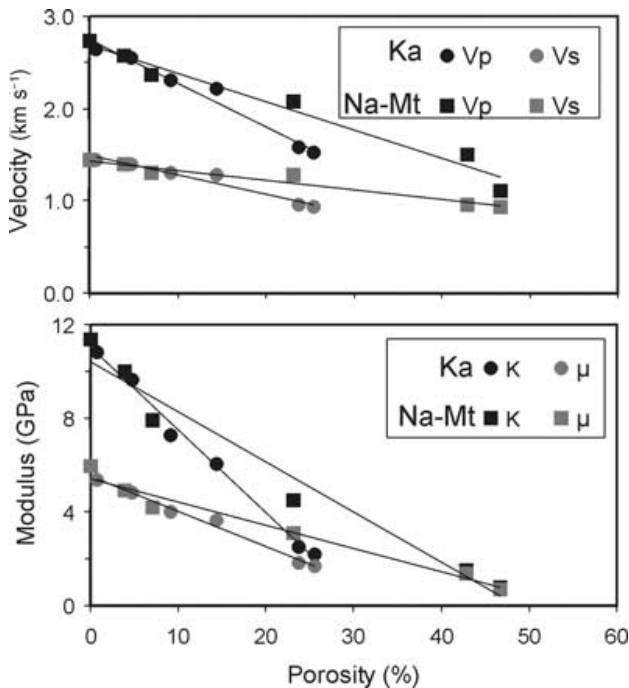
Figure 6. Velocity (a) and elastic moduli (b) as functions of porosity from uniaxial stress tests for kaolinite (Ka, filled circles) and Na-montmorillonite (Na-Mt, crosses) in dry conditions. Lines show linear fits to the data: $M = a\Phi + b$. The error on velocity is 1 per cent; the error bar in the velocity plots is smaller than the size of symbols used.
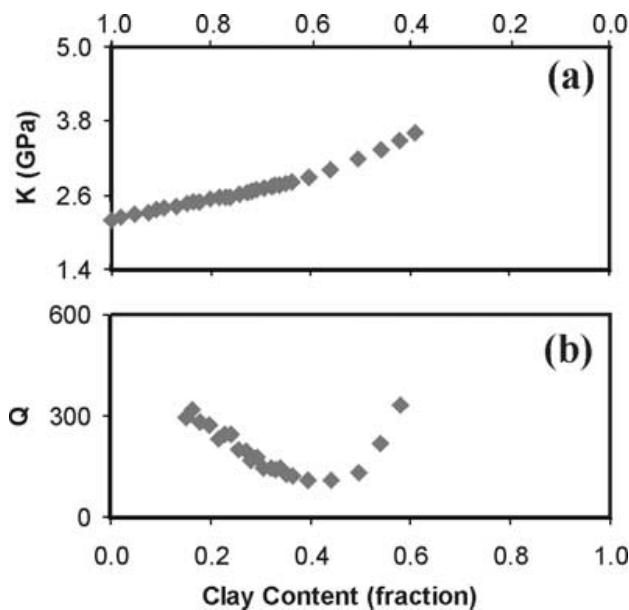

Figure 7. Bulk modulus (a) and *P*-wave quality factor (b) as functions of clay content in a kaolinite–KCl suspension.

dispersed in the pore space of the load-bearing clay. Above this point, the increased stiffness due to the clay outweighs density and scattering effects and both K and Q_p increase with increasing clay content. Note that although degassing under vacuum was problematic above 40 per cent clay content, we do not expect a significant quantity of gas bubbles to be present. The presence of gas in the

suspension would lower V_p and it would lower Q_p significantly. The increase in Q_p at clay concentrations larger than 40 per cent (Fig. 7b) suggests that gas concentrations were negligible.

4 VELOCITY MODELLING

Both of our experiments on cold-pressed samples gave consistent values of bulk modulus in the range 6–11 GPa and of shear modulus in the range 4–6 GPa that agree with the measurements of Prasad *et al.* (2002). We first compare our results with those reported by Katahara (1996), Wang *et al.* (2001) and Prasad *et al.* (2002) by using them as input in the Hashin–Shtrikman (HS) model (Hashin & Shtrikman 1963) and the modified Voigt average (MVA) (Nur *et al.* 1991, 1998) to calculate the bulk modulus of a kaolinite–water suspension. K_{water} was taken as 2.2 GPa (Mavko *et al.* 1998). Note that in a homogeneous fluid suspension, where $\mu = 0$, the Hashin–Shtrikman lower bound is equivalent to the isostress Reuss average (K_{reuss}) of the composite given by

$$\frac{1}{K_{reuss}} = \sum_{i=1}^{N} \frac{f_i}{K_i}, \tag{1}$$

where N is the number of components and f_i is the fraction of the component.

In Fig. 8, Hashin–Shtrikman upper and lower bounds (HS^+ and HS^-, respectively) of the bulk modulus (Hashin *et al.* 1963) and the modified Voigt average (Nur *et al.* 1991, 1998) of a water–clay mixture are compared with experimental measurements in saturated kaolinite samples (Yin 1993) and in kaolinite–water suspensions (this study). In Fig. 8(a), the calculations were made using 12 and 6 GPa for the bulk and shear moduli of the solid phase, K_s and μ_s, respectively, (Prasad *et al.* 2002, this study). Calculations with $K_s = 56$ and $\mu_s = 32$ GPa (Katahara 1996) and $K_s = 47.9$ and $\mu_s = 19.7$ GPa (Wang *et al.* 2001) are shown in Fig. 8(b). In Fig. 8(a), the lower HS^- bound lies on the values measured in the kaolinite–water suspensions and the modified Voigt average predictions agree with measurements in the saturated kaolinite sample from Yin (1993). These predictions support the conceptual first-principles-based model of Dvorkin *et al.* (1999) and Prasad & Dvorkin (2001), wherein the softer material (water) is load-bearing above critical porosity (Φ_c) (Nur *et al.* 1998) and the system is adequately described by the lower HS bound. Once the stiffer material (clay) becomes load-bearing, as in the saturated kaolinite sample, the measured velocity values move away from the lower HS bound and are better predicted by the modified Voigt average. As described in Nur *et al.* (1998), critical porosity separates the domain in which a rock sample is frame-supported ($\Phi_{sample} < \Phi_c$) from that in which it is fluid-supported ($\Phi_{sample} > \Phi_c$).

The higher values of bulk and shear moduli from Katahara (1986) and Wang *et al.* (2001), respectively, overpredict experimental measurements both for kaolinite–water suspensions and for kaolinite samples (Fig. 8b).

As a second test, we calculated V_p in shaley sandstones using the different K_s and μ_s values as above for clay and $K_s = 36.6$ GPa and $\mu_s = 45$ GPa for quartz (Mavko *et al.* 1998). Han *et al.* (1986) have shown that the velocity in sandstones is dependent on the porosity and on the clay content: at the same porosity, clay-rich sandstones have a lower velocity than clean sandstones. Theoretical velocities calculated with the rock physics model reported in Dvorkin *et al.* (1999) and Prasad & Dvorkin (2001) are compared with velocities measured on clean and clay-rich sandstones at 40 MPa confining pressure (Tosaya 1982; Han *et al.* 1986; Klimentos 1991) in Fig. 9. This model uses the Hertz–Mindlin (Mindlin
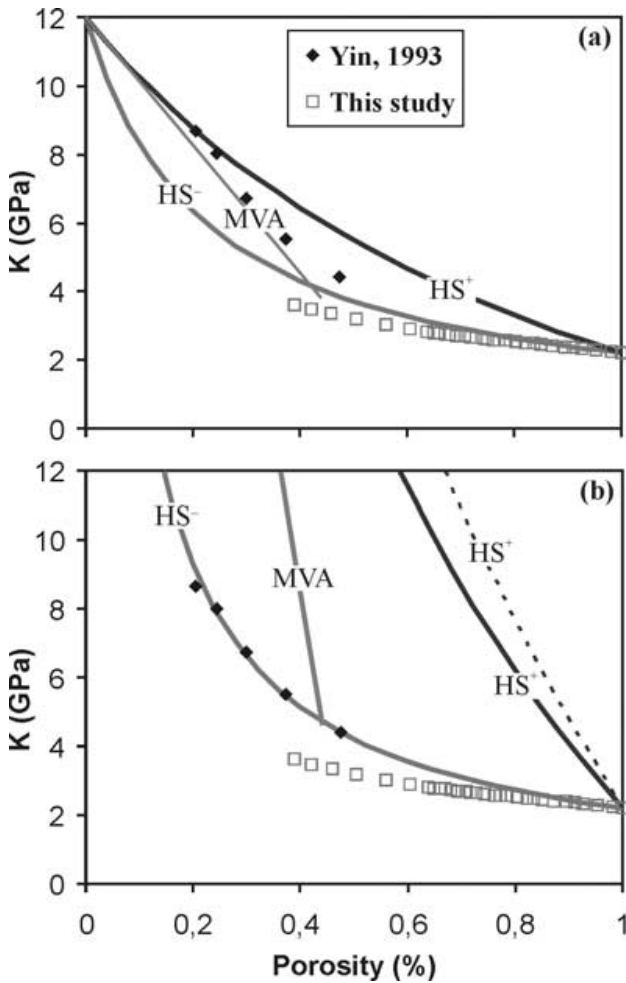
Figure 8. Hashin–Shtrikman lower and higher bounds (HS⁻ and HS⁺, respectively) and the modified Voigt average compared with experimental measurements in saturated kaolinite samples (black diamonds; Yin 1993) and kaolinite suspension (open squares; this study). (a) Elastic clay moduli for theoretical curves taken from the uniaxial stress experiment and (b) values taken from literature Katahara (1996) marked by dotted line and Wang *et al.* (2001) marked by solid line.

Figure 9. *P*-wave velocity as a function of porosity for shaley sandstones at 40 MPa. The experimental data from Tosaya (1982), Han (1986), Klimentos (1991), are shown by symbols coded by clay content. Data are compared with modelling described in Dvorkin *et al.* (1999) and Prasad & Dvorkin (2001): solid lines mark the upper bounds (HS^{HM+}), dotted lines mark lower bounds (HS^{HM-}). Elastic clay moduli used to generate theoretical curves were taken from values measured by the uniaxial stress experiment (a) and literature values (Katahara 1996; Wang *et al.* 2001) (b).

nificant modulus reduction with increasing clay content. Using the moduli obtained from this study and from Prasad *et al.* (2002), we obtain a much better agreement between model prediction and experimental data (Fig. 9a) Fig. 9(a) shows that the lower moduli of clay explains both the reduction of the velocity as a function of clay content and the separation in measured velocities due to addition of clay to the sandstones.

5 CONCLUSIONS

We have measured elastic moduli values between 6 and 12 GPa for bulk (K_s) and between 4 and 6 GPa for shear (μ_s) in kaolinite, montmorillonite and smectite clay minerals. These results, obtained using different sample preparation and measurements techniques are consistent with one other and those obtained with atomic force acoustic microscopy by Prasad *et al.* (2002). They are also comparable to values extrapolated and modelled from laboratory and log measurements on shales (Han 1986; Castagna *et al.* 1995; Berge & Berryman 1995).

Note that our measurements are much lower than the theoretical extrapolations of Katahara (1996) and measurements on clay–epoxy mixtures (Wang *et al.* 2001). We suggest that a possible reaction between clay minerals and the polar organic epoxy fluid might lead to a super-dry clay with a higher mineral modulus.

In addition to the consistency check, we modelled the elastic moduli in binary systems: porous clay-quartz and water–kaolinite.

1949) contact theory to compute first the effective bulk (K_{HM}) and shear (μ_{HM}) moduli of a dry mixture of quartz and clay at critical porosity (Φ_c) (Nur *et al.* 1998) under a given pressure. Next, the upper and lower Hashin–Shtrikman bounds (HS$^{HM\pm}$) (1963) are calculated between the two end-points at zero porosity (K_S, μ_S) and at the critical porosity (K_{HM}, μ_{HM}) for this two-component mixture of quartz and clay. Finally, the elastic moduli of water-saturated clay–quartz mixture are calculated using Gassmann's fluid substitution equations (see Dvorkin *et al.* 1999; Prasad & Dvorkin 2001, for details). As in Fig. 8, Fig. 9(a) shows theoretical curves for the clay mineral moduli, $K_s = 12$ GPa and $\mu_s = 6$ GPa and Fig. 9(b) for $K_s = 47.9$ GPa and $\mu_s = 19.7$ GPa. Figs 9(a) and (b), show theoretical curves computed for clay contents values of 5, 15, 25 and 50 per cent. The computations show that in a two-phase system, if the individual phases have similar elastic moduli, then increasing the concentration of one phase over the other will not alter the moduli of the composite system. Thus, in Fig. 9(b), since the moduli of clay ($K_s = 47.9$ GPa and $\mu_s = 19.7$ GPa) and quartz ($K_s = 36.6$ GPa and $\mu_s = 45$ GPa) are very similar, the model does not predict a sig-
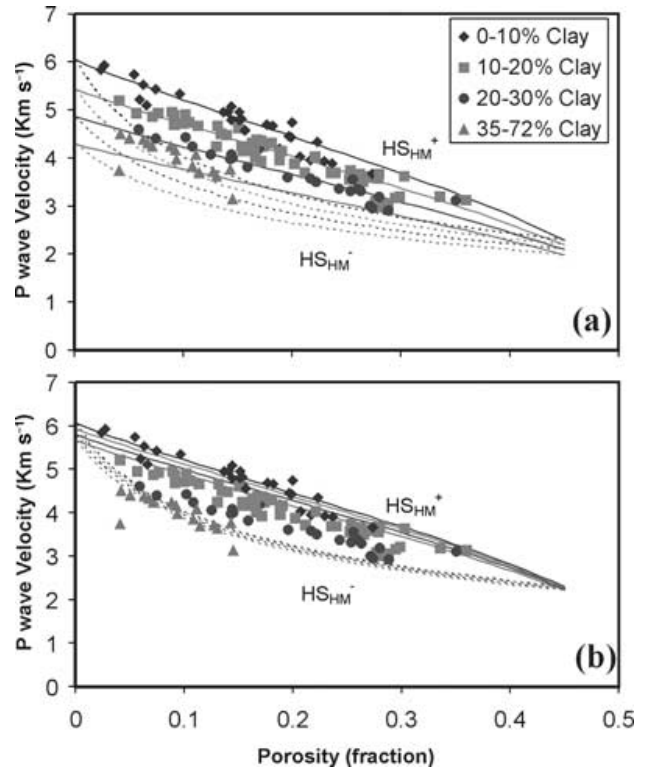
We used values measured in this study and those from Katahara (1996) and Wang *et al.* (2001) for clay mineral moduli. Using $K_s = 12$ GPa and $\mu_s = 6$ GPa from this study, the model gives a much better prediction both of experimental velocity reduction due to increase in clay content in sandstones and velocity measurements in a kaolinite–water suspension.

ACKNOWLEDGMENTS

REFERENCES

Alexandrov, K.S. & Ryzhova, T.V., 1961. Elastic properties of rock-forming minerals II. Layered silicates, *Bull. USSR Acad. Sci., Geophys. Ser.,* **9,** 1165–1168.

ASTM, 1992. Standard specifications for grain density determination of soils, *ASTM Designation D854–92,* American Society for Testing Materials.

Berge, P.A. & Berryman, J.G., 1995. Realizability of negative pore compressibility in poroelastic composites, *J. Appl. Mech.,* **62,** 1053–1062.

Brace, W.F., Scholtz, C.H. & La Mori, P.N., 1969. Isothermal compressibility of kayanite, andalusite, and sillimanite from synthetic aggregates, *J. geophys. Res.,* **74,** 2089–2098.

Castagna, J.P., Han, De-hua & Batzle, M.L., 1995. Issues in rock physics and implications for DHI interpretation, *The Leading Edge,* **14,** 883–885.

Chung, D.H., 1979. Elasticity of Stishovite revisited, in *High Pressure Science and Technology,* eds Timmerahaus, K.D. & Baber, M.S., Plenum, New York.

Colten Bradley, V.A., 1987. Role of pressure in smectite dehydration-effects on geopressure and smectite-to-illite transformation, *AAPG Bull.,* **71,** 1414–1427.

Dvorkin, J., Prasad, M., Sakai, A. & Lavoie, D., 1999. Elasticity of marine sediments: rock physics modeling, *Geophys. Res. Lett.,* **26,** 1781–1784.

Eastwood, R.L. & Castagna, J.P., 1987. Interpretation of V_p/V_s ratios from sonic logs, *Geophys. Develop.,* **1,** 139–153.

Han, De-hua, 1986. Effects of porosity and clay content on acoustic properties of sandstones and unconsolidated sediments, *PhD dissertation,* Stanford University, Stanford.

Han, De-hua, Nur, A. & Morgan F.D., 1986. The events of porosity and clay content on wave velocities in sandstones, *Geophysics,* **51,** 2093–2107.

Hashin, Z. & Shtrikman, S., 1963. A variational approach to the elastic behaviour of multiphase materials, *J. Mech. Phys. Solids,* **11,** 127–140.

Katahara, K.W., 1996. Clay mineral elastic properties, *SEG Annual Meeting Expanded Technical Programme Abstracts,* Paper RP1.4.

Klimentos, T., 1991. The effects of porosity–permeability–clay content on the velocity of compressional waves, *Geophysics,* **56,** 1930–1939.

Koster Van Groos, A.F. & Guggenheim, S., 1984. The effect of pressure on the dehydration reaction of interlayer water in Na-montmorillonite (SWy-1), *Am. Mineralog.,* **69,** 9–10, 872–879.

Kowallis, B.J., Jones, L.E.A. & Wang, H.F., 1984. Velocity–porosity–clay content systematics of poorly consolidated sand-stones, *J. geophys. Res.,* **89,** 10 355–10 364.

Marion, D., Nur, A., Yin, H. & Han, D., 1992. Compressional velocity and porosity in sand–clay mixtures, *Geophysics,* **57,** 554–363.

Mavko, G., Mukerjy, T. & Dvorkin, J., 1998. *Rock Physics Handbook,* Cambridge University Press, Cambridge.

Mindlin, R.D., 1949. Compliance of elastic bodies in contact, *Trans. ASME,* **71,** A-259.

Newman, A.C.D., 1987. *Chemistry of Clays and Clay Minerals,* Vol. 6, p. 480, Mineralogical Society, London.

Nur, A., Marion, D. & Yin, H., 1991. Wave velocities in sediments, in *Shear Waves in Marine Sediments,* pp. 131–140, eds Hovem, J.M. *et al.*, Kluwer, Dordrecht.

Nur, A., Mavko, G., Dvorkin, J. & Galmudi, D., 1998. Critical porosity: a key to relating physical properties to porosity in rocks, *The Leading Edge,* **17,** 357–362.

Prasad, M. & Manghnani, M.H., 1997. Effects of pore and differential pressures on compressional wave velocity and quality factor on Berea and Michigan sandstones, *Geophysics,* **62,** 1163–1176.

Prasad, M. & Dvorkin, J., 2001. Velocity to porosity transforms in marine sediments, *Petrophysics,* **42,** 429–437.

Prasad, M., Kopycinska, M., Rabe, U. & Arnold, W., 2002. Measurement of Young's modulus of clay minerals using atomic force acoustic microscopy, *Geophys. Res. Lett.,* **29,** 8.

Theng, B.K.G., 1974. *The Chemistry of Clay–Organic Reactions,* p. 343, Hilger, London.

Toksöz, M.N., Johnston, D.H. & Timur, A., 1979. Attenuation of seismic waves in dry and saturated rocks, I. Laboratory measurements, *Geophysics,* **44,** 681–690

Tosaya, C.A., 1982. Acoustical properties of clay bearing rocks, *PhD dissertation,* Stanford University, Stanford.

Tosaya, C.A. & Nur, A., 1982. Effect of diagenesis and clays on compressional velocities in rocks, *Geophys. Res. Lett.,* **9,** 5–8.

Vanorio, T., Prasad, M., Patella, D. & Nur, A., 2002. Ultrasonic velocity measurements in volcanic rocks: correlation with microtexture, *Geophys. J. Int.,* **149,** 22–36.

Wang, Z., Wang, H. & Cates, M.E., 2001. Effective elastic properties of solid clays, *Geophysics,* **66,** 428–440.

Yin, H., 1993. Acoustic velocity and attenuations of rocks: isotropy, intrinsic anisotropy, and stress induced anisotropy, *PhD dissertation,* Stanford University, Stanford.